Size-Controlled Growth of Co_3O_4 Nanocubes

Ji Feng and Hua Chun Zeng*

Department of Chemical and Environmental Engineering, Faculty of Engineering, National University of Singapore, 10 Kent Ridge Crescent, Singapore 119260

Received September 24, 2002. Revised Manuscript Received December 23, 2002

Recently we investigated a nitrate-salt-mediated formation route of Co_3O_4 spinel nanocubes with a uniform size of ca. 47 nm in aqueous solution at 95 °C (*J. Phys. Chem. B* **2003**, *107* (4), 926−930). In the present work, we examined various synthetic parameters of this new method. By varying reaction temperature and time, the size control of Co_3O_4 nanocubes has been achieved, which produces the spinel nanocubes with a controllable edge length in the regime of 10−100 nm. A linear relationship between the cube size and reaction time has been revealed. Furthermore, a process has been developed to separate (or to purify) the growing Co_3O_4 nanocubes from remaining solid products at different synthetic stages. With a large amount of nitrate salt added, we have been able to observe some irregular crystalline intermediates, although the majority of the Co_3O_4 nanocrystals have highly symmetrical cubelike morphology. On the basis of the observed crystallite morphologies, we have elucidated in this work a mechanism — "surface wrapping" — to describe the size-controlled growth of Co_3O_4 nanocubes.

Introduction

Nanometer-scale materials with the size of 1−100 nm have attracted considerable interest in recent years due to the departure of properties from bulk phases arising from quantum size effect.[1] Over the past decade, a variety of techniques have been applied to fabricate nanostructures of a broad class of materials, ranging from ceramic dielectrics,[2,3] semiconductors,[4,5] metals,[6,7] metal oxides and sulfides (e.g., metal dichalcogenides nanotubes),[8−13] and metal hydroxides[14−16] to the most studied fullerene-carbons (e.g., carbon nanotubes).[17−19] These nanostructures possess diverse morphologies, including zero-dimensional (0D) quantum dots, one-dimensional (1D) quantum wires, and other two-dimensional (2D) layered structures with a high degree of symmetry.[1−21] It is now commonly understood that the behaviors of nanophase materials strongly depend on the shapes and sizes of the particles, which are thus a key factor to their ultimate performance and applications. In this regard, it is desirable to tailor-synthesize nanoparticles with pre-designed morphology and size distributions.[22]

Unitary spinel cobalt oxide (Co_3O_4) stands as an important functional material, in part because of its vast applications for use in pigments, catalysis, sensors, electrochemistry, magnetism, and energy storage (e.g., intercalation compounds for battery materials).[23−25]

* To whom correspondence should be addressed. E-mail: chezhc@nus.edu.sg.

(1) Hook, J. R.; Hall, H. E. *Solid State Physics*, 2nd ed.; John Wiley & Sons Ltd.: Chichester, U.K., 1991; Chapter 14.
(2) Ishikawa, T.; Yamaoka, H.; Harada, Y.; Fujii, T.; Nagasawa, T. *Nature* **2002**, *416*, 64.
(3) Liu, C.; Zou, B.; Rondinone, A. J.; Zhang, Z. J. *J. Am. Chem. Soc.* **2001**, *123*, 4344.
(4) Penn, R. L.; Banfield, J. F. *Science* **1998**, *281*, 969.
(5) (a) Huang, M. H.; Wu, Y. Y.; Feick, H.; Tran, N.; Weber, E.; Yang, P. D. *Adv. Mater.* **2001**, *13*, 113. (b) Huang, M. H.; Mao, S.; Feick, H.; Yan, H.; Wu, Y.; Kind, H.; Webber, E.; Russo, R.; Yang, P. *Science* **2001**, *292*, 1897.
(6) Rao, C. N. R.; Kulkarni, G. U. K.; Thomas, P. J.; Edwards, P. P. *Chem. Soc. Rev.* **2000**, *29*, 27, and references therein.
(7) (a) Hong, B. H.; Bae, S. C.; Lee, C.-W.; Jeong, S.; Kim, K. S. *Science* **2001**, *294*, 348. (b) Kim, B.; Tripp, S. L.; Wei, A. *J. Am. Chem. Soc.* **2001**, *123*, 7955.
(8) Poizot, P.; Laruelle, S.; Grugeon, L. D.; Tarascon, J. M. *Nature* 407, *496*.
(9) Matijević, E. *Chem. Mater.* **1993**, *5*, 412, and references therein.
(10) Tonguzzo, P.; Viau, G.; Acher, O.; Fiévet-Vincent, F.; Fiévet, F. *Adv. Mater.* **1998**, *10* (13), 1032.
(11) Xia, B.; Lenggoro, I.; Okuyama, K. *Adv. Mater.* **2001**, *13* (20), 1579.
(12) Agnoli, F.; Zhou, W. L.; O'Connor, C. J. *Adv. Mater.* **2001**, *13* (22), 1697.
(13) (a) Tenne, R.; Margulis, M.; Genut, M.; Hodes, G. *Nature* **1992**, *360*, 444. (b) Tenne, R.; Homyonfer, M.; Feldman, Y. *Chem. Mater.* **1998**, *10*, 3225. (c) Zak, A.; Alperovich, V.; Rosentsveig, R.; Tenne, R. *J. Am. Chem. Soc.* **2000**, *122*, 11108. (d) Feldman, Y.; Homyonfer, M.; Lyakhovitskaya, V.; Margulis, L.; Cohen, H.; Hutchson, J. L.; Tenne, R. *J. Am. Chem. Soc.* **1996**, *118*, 5362.
(14) (a) Ding, Y.; Zhang, G.; Wu, H.; Hai, B.; Wang, L.; Qian, Y. *Chem. Mater.* **2001**, *13*, 435. (b) Li, Y.; Sui, M.; Ding, Y.; Zhang, G.; Zhuang, J.; Wang, C. *Adv. Mater.* **2000**, *12*, 818.
(15) Salvadori, B.; Dei, L. *Langmuir* **2001**, *17*, 2371.
(16) Sampanthar, J. T.; Zeng, H. C. *J. Am. Chem. Soc.* **2002**, *124*, 6668.
(17) (a) Iijima, S. *Nature* **1991**, *354*, 56. (b) Ajayam, P. M.; Iijima, S. *Nature* **1992**, *358*, 23.
(18) (a) Ebbesen, T. W.; Ajayan, P. M. *Nature* **1992**, *358*, 220. (b) Banhart, F.; Ajayan, P. M. *Nature* **1996**, *382*, 433. (c) Ajayan, P. M. *Chem. Rev.* **1999**, *99*, 1787, and references therein.
(19) Thess, A.; Lee, R.; Nikolaev, P.; Dai, H.; Petit, P.; Robert, J.; Xu, C.; Lee, Y. H.; Kim, S. G.; Rinzler, A. G.; Colbert, D. T.; Scuseria, G. E.; Tomanek, D.; Fischer, J. E.; Samalley, R. E. *Science* **1996**, *273*, 483.
(20) Niemeyer, C. M. *Angew. Chem., Int. Ed.* **2001**, *40*, 4128, and references therein.
(21) (a) Choy, J. H.; Kwak, S. Y.; Park, J. S.; Jeong, Y. J.; Portier, J. *J. Am. Chem. Soc.* **1999**, *121*, 1399. (b) Choy, J. H.; Kwak, S. Y.; Jeong, Y. J.; Park, J. S. *Angew. Chem., Int. Ed.* **2000**, *39* (22), 4041.
(22) Cheung, C. L.; Kurtz, A.; Park, H.; Lieber, C. M. *J. Phys. Chem. B* **2002**, *106*, 2429.
(23) (a) Ocana, M.; Gozalez-Elipe, A. R. *Colloids Surf., A* **1999**, *157*, 315. (b) Barreca, D.; Massignan, C.; Daolio, S.; Fabrizio, M.; Piccirillo, C.; Armelao, L.; Tondello, E. *Chem. Mater.* **2001**, *13*, 588. (c) del Barco, E.; Asenjo, J.; Zhang, X. X.; Pieczynski, R.; Julia, A.; Tejada, J.; Ziolo, R. F.; Fiorani, D.; Testa, A. M. *Chem. Mater.* **2001**, *13*, 1487.

10.1021/cm020940d CCC: $25.00
Published on Web 06/06/2003

Spinel Co_3O_4, when falling in the nanosized regime, is expected to lead to even more attractive applications in the conjunction of their traditional arena and nanotechnology. Therefore, it would be highly desirable to prepare nanocrystals of spinel cobalt oxide with well-defined morphologies and a narrow range of size distribution. Transition metal spinels are conventionally synthesized by a solid-state reaction of mixed metal salts at elevated temperatures.[26] However, extremely active atomic vibration at high reaction temperature usually leads to sintering and/or grain growth, rendering this route unlikely to produce nanoparticles. Many new techniques have also been devised for the spinel synthesis so as to make low-temperature synthesis possible. In recent years, preparations of single-phase Co_3O_4 at temperatures ranging from 150 to 260 °C have been made via spray pyrolysis, chemical vapor deposition, and sol−gel routes.[27−29] It has also been reported that Co_3O_4 can be formed at 70−100 °C from a precursor compound cobalt(III) hydroxyoxide (CoOOH).[24,26b,30,31] In particular, as early as 1978, monodispersed cubic Co_3O_4 (~0.1 μm edge length) had been synthesized through a "forced hydrolysis" method at 100 °C starting with highly dilute cobaltous acetate solutions.[24] The same method, however, was reportedly unproductive if starting with $Co(NO_3)_2$ salt.[24]

It is vitally important to study the fundamentals of nanocrystalline Co_3O_4 spinel formation with various synthetic routes because the understanding of this aspect will guide us to newer materials design and more sophisticated synthetic methods. Despite the research activities discussed above, work that leads to the knowledge of their formation and growth mechanisms is still essentially lacking. Very recently, we developed a synthetic method for fabrication of free-standing nanocubic Co_3O_4 via a "soft" chemical route at 95 °C.[32] Unlike the previously reported approach,[24] we added a large amount of sodium nitrate to mediate the Co_3O_4 synthesis. Our mechanistic phase investigation indicated that there are various precursor compounds formed prior to the resultant Co_3O_4 phase:[32] starting from β-$Co(OH)_2$ (brucite-like structure), cobalt(II) hydroxide-nitrate $Co^{II}(OH)_{2-x}(NO_3)_x \cdot nH_2O$ ($x \approx 0.2-0.5$, $n \approx 0.1$; also a layered compound),[33] and hydrotalcite-like layered-double-hydroxide $Co^{II}_{1-x}Co^{III}_x(OH)_2(NO_3)_x \cdot nH_2O$ ($x \approx 0.26-0.28$, $n \approx 0.3-0.6$).[34] With this approach, single-crystalline Co_3O_4 particles with a perfect cubic shape and an average size of 47 nm were fabricated.

In the present work, as a continued part of our research endeavor in this area, we will report our new research findings in size-controlled growth of Co_3O_4 nanocubes. In particular, we have achieved size control of these Co_3O_4 nanocubes in the special regime of 10−100 nm by varying the reaction temperature and time. With new investigations on the salt-mediated growth (by adding nitrate salt), we have also been able to observe intermediate crystallites of Co_3O_4 prior to their final nanocube morphology. On the basis of the arrested intermediates, a "surface wrapping" growth mechanism, which leads to the formation of cubical morphology, has been discovered.

Experimental Section

Sample Preparation. In a typical synthesis, 1.2 g of NaOH (30 mmol, Merck, >99.0%) was dissolved in 100.0 mL of deionized water in a three-necked round-bottom flask. Then 90−150 g of $NaNO_3$ (1059−1765 mmol, Merck, >99.5%) was added to the solution. The three-necked flask, with a reflux condenser mounted on top, was then immersed into an oil bath at 105 ± 0.2 °C. A purified air stream (50 mL/min, Soxal, O_2 = 21 ± 1%, H_2O <2 volume per million (vpm) and hydrocarbons <5 vpm) was continuously bubbled through the solution. After half an hour, 20.0 mL of 1.0 M $Co(NO_3)_2 \cdot 6H_2O$ (20 mmol, Merck, >99.0%) was added dropwise within 1 min using a buret. Blue precipitate formed instantaneously. The flask with the blue slurry was kept in the oil bath for further reaction (i.e., aging at 105 °C). The whole process was carried out under constant stirring by a magnetic stirrer. At different aging times, a small amount of slurry was drawn from the reaction vessel by using an auto-pipet. The slurry was naturally cooled in ambient condition to room temperature and then centrifuged at 3000 rpm for 20 min. After removal of the supernatant, the solid was re-suspended in a 2.0 M HCl solution to dissolve unreacted precursor compounds (β-$Co(OH)_2$, $Co^{II}(OH)_{2-x}(NO_3)_x \cdot nH_2O$, and $Co^{II}_{1-x}Co^{III}_x(OH)_2(NO_3)_x \cdot nH_2O$). The mixture was then centrifuged again. This was repeated four times to ensure complete removal of the precursor phases. The black paste (purified Co_3O_4) left in the centrifuge tubes was re-suspended in deionized water and recentrifuged. This later washing was also repeated four times.

Material Characterization. *XRD Measurement.* Powder XRD measurement was carried out to obtain phase information. The XRD patterns of diffraction intensity as a function of 2θ were collected using a Shimadzu X-ray diffractometer (model 6000) with Cu Kα radiation (λ = 1.5406 Å) from 5° to 80° at a scanning rate of 2°/min. The X-ray tube voltage and current were set at 40 kV and 30 mA, respectively.

TEM Measurement. Investigations on morphology of the Co_3O_4 nanocrystallites and their electron diffractions (ED) were carried out using a high-resolution transmission electron microscope (HRTEM, JEOL, JEM-2010). The electron beam accelerating voltage was set at 200 kV and the current was set at 106 mA. The solid sample was first suspended in deionized water by sonication in an ultrasonic water bath for an hour. A drop of this well-dispersed suspension was then applied on a piece of 200-mesh carbon-coated copper grid, followed by air-drying under ambient condition before the copper grid was placed into the TEM specimen holder.

Thermal Analysis. About 12−14 mg of each sample was analyzed using a thermogravimetric and differential-thermogravimetric analyzer (TGA/DTG, Shimadzu TGA-50). The sample was loaded into a platinum crucible that was then heated in the TGA furnace from room temperature to 950 °C

(24) Sugimoto, T.; Matijević, E. *J. Inorg. Nucl. Chem.* **1978**, *41*, 165.
(25) (a) Zeng, H. C.; Lin, J.; Tan, K. L. *J. Mater. Res.* **1995**, *10*, 3096. (b) Zeng, H. C.; Lim, Y. Y. *J. Mater. Res.* **2000**, *15*, 1250. (c) Ji, L.; Lin, J.; Zeng, H. C. *J. Phys. Chem. B* **2000**, *104*, 1783.
(26) (a) Sakamoto, S.; Yoshinaka, M.; Hirota, K.; Yamaguchi, O. *J. Am. Ceram. Soc.* **1997**, *80*, 267. (b) Jang, Y.-I.; Wang, H.; Chiang, Y.-M. *J. Mater. Chem.* **1998**, *8*, 2761.
(27) Baydi, M. E.; Poillerat, G.; Rehspringer, J.-L.; Gautier, J. L.; Koenig, J.-F.; Chartier, P. *J. Solid State Chem.* **1994**, *109*, 281.
(28) Fujii, E.; Torii, H.; Tomozawa, A.; Takayama, R.; Hirao, T. *J. Mater. Sci.* **1995**, *30*, 6013.
(29) Gautier, J. L.; Rios, E.; Gracia, M.; Marco, J. F.; Gancedo, J. R. *Thin Solid Films* **1997**, *311*, 51.
(30) Rojas, R. M.; Vila, E.; Garcia, O.; Martin de Vidales, J. L. *J. Mater. Chem.* **1994**, *4*, 1635.
(31) Furlanetto, G.; Formado, L. *J. Colloid Interface Sci.* **1995**, *170*, 169.
(32) Xu, R.; Zeng, H. C. *J. Phys. Chem. B* **2003**, *107* (4), 926−930.
(33) (a) Rajamathi, M.; Kamath, P. V.; Seshadri, R. *Mater. Res. Bull.* **2000**, *35*, 271. (b) Rajamathi, M.; Thomas, G. S.; Kamath, P. V. *Proc. Indian Acad. Sci. (Chem. Sci.)* **2001**, *113*, 671. (c) Zotov, N.; Petrov, K.; Dimitrova-Pankova, M. *J. Phys. Chem. Solids* **1990**, *51*, 1199. (d) Effenberger, H. *Z. Kristallogr.* **1983**, *165*, 127.
(34) (a) Xu, Z. P.; Zeng, H. C. *J. Mater. Chem.* **1998**, *8*, 2499. (b) Xu, Z. P.; Zeng, H. C. *Chem. Mater.* **1999**, *11*, 67. (c) Xu, Z. P.; Zeng, H. C. *Chem. Mater.* **2000**, *12*, 3459.

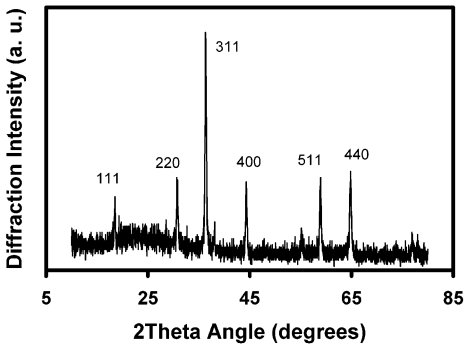

Figure 1. Powder XRD pattern of single-crystalline Co_3O_4 nanocubes prepared in this work (12 h aging, 120 g of $NaNO_3$ salt used in this synthesis).

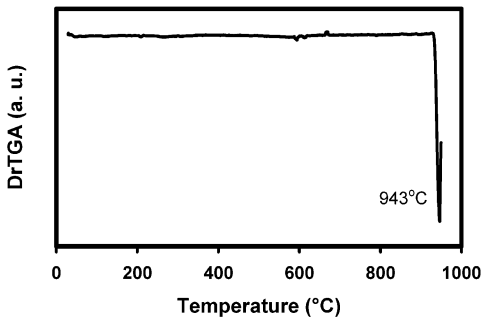

Figure 2. Differential TGA (DrTGA) curve of Co_3O_4 nanocubes (12 h aging, 120 g of $NaNO_3$ salt used in this synthesis) in purified air stream (50 mL/min) at a heating rate of 10 °C/min.

at a rate of 10 °C/min. A purified air stream (50 mL/min, as specified before) was passed through the furnace throughout the programmed heating.

Results and Discussion

Structural and Compositional Analysis. Figure 1 shows a representative XRD pattern of samples prepared with this approach, which indicates that all the products are phase-pure crystalline Co_3O_4 (in cubic symmetry; space group (SG) *Fd*3*m*, lattice constant $a = 0.8084$ nm).[35] Our previous investigation indicated that the material obtained without purifying with hydrochloric acid was in fact a mixture of Co_3O_4 and cobalt hydroxide and hydroxide nitrates with divalent or mixed valencies (e.g., β-$Co(OH)_2$, $Co^{II}(OH)_{2-x}(NO_3)_x \cdot nH_2O$, and $Co^{II}{}_{1-x}Co^{III}{}_x(OH)_2(NO_3)_x \cdot nH_2O$) when the aging times were shorter than 24 h at 95 °C.[32] With the synthetic temperature 105 °C used in this work, the conversion of these precursor phases turns out to be much more efficient. The well-resolved diffraction peaks in Figure 1 reveal the good crystallinity of the Co_3O_4 specimens. The composition of resultant Co_3O_4 is further confirmed by our TGA measurement. The differential TGA curve of Figure 2 shows that there is no weight loss until the temperature reaches about 940 °C. The rapid weight loss corresponding to the peak at 943 °C is associated with the thermal decomposition of Co_3O_4 in air atmosphere:[34]

$$Co_3O_4 = 3\ CoO + {}^1/_2\ O_2\uparrow \qquad (1)$$

The presence of the above hydroxides residue can be ruled out because they decompose at temperatures well below 940 °C; their existence should have given rise to additional peaks in the differential TGA cruve.[34] Therefore, the acidic purification technique with HCl proves to be successful in removing the hydroxides residue and yet preserving the spinel oxide Co_3O_4. This technique becomes even more crucial when manipulating the size of the spinel oxide particles, which will be discussed shortly.

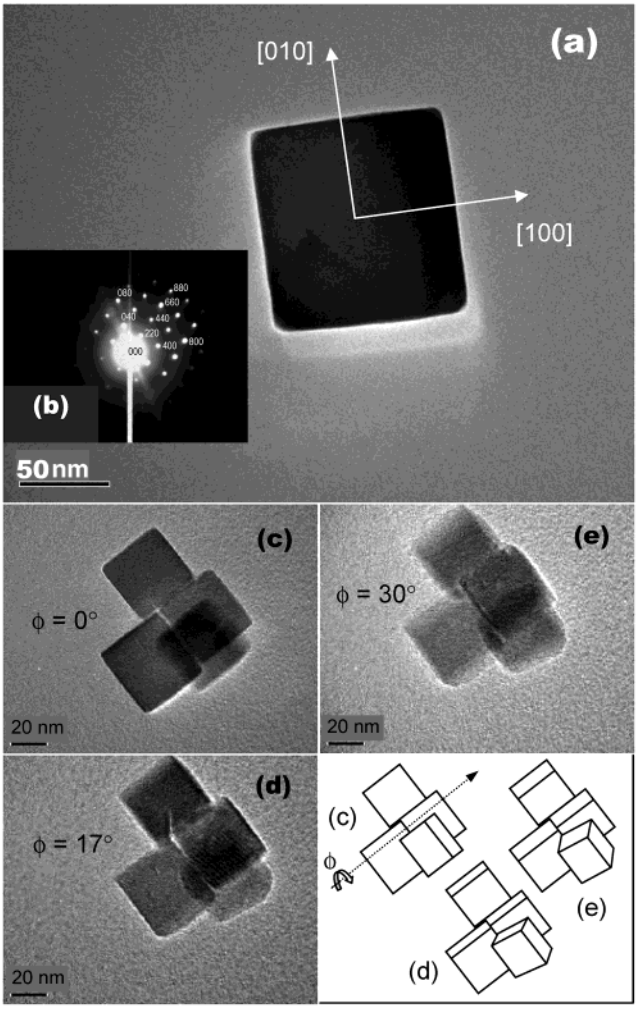

Figure 3. TEM images and electron diffraction pattern of Co_3O_4 nanocubes obtained in this work: (a) single-crystal Co_3O_4 nanocube (24 h aging and 90 g of sodium nitrate used); (b) ED pattern of (a); and (c) to (e) TEM images of four nanoparticles (12 h aging and 150 g of sodium nitrate used); ϕ is the angle over which the copper grid was tilted.

Morphology of Co_3O_4 Nanocubes. As reported in Figure 3, the above-prepared Co_3O_4 products have perfect cubic morphology. Excellent crystallinity of Co_3O_4 nanocubes is also confirmed with our ED experiment. Figure 3b shows a spot pattern from a Co_3O_4 single-crystal cube (Figure 3a). In this case, the electron beam is incident along the [001] direction, and the spot array has a 4-fold axis that can be indexed with *hk*0 (i.e., [001] zone spots, in accordance to the extinction rule of electron diffraction of SG *Fd*3*m*), indicating a cubic symmetry for Co_3O_4 nanocubes. Reported in Figure 3c and d are the TEM images of four Co_3O_4

(35) Joint Committee on Powder Diffraction Standards, International Centre for Diffraction Data. Card 43-1003; Swarthmore, PA, 1996.

nanoparticles prepared after aging for 12 h. It is clear that the projection views of most particles are square in shape. Three particles, free-standing on their {001} faces, are self-aligned according to their magnetic-dipoles, whereas the remaining one leans on its cube edge ([110] direction). To confirm the morphology of these cubic particles, tilted TEM investigation was carried out to obtain the transmission images from different viewing angles. The first image is that of the particles prior to tilting ($\phi = 0°$) with perfect square shape, uniform resolution, and clear-cut edges. When the copper grid was tilted with an angle of $\phi = 17-30°$, it is observed that the images of the particles are elongated and there is a transition of contrast along the direction of elongation. The center is apparently darker than the tilted edges. The edges become fuzzy when ϕ increases, because of the shortening travel distance for penetrating electrons. All these observations confirm that the particles are indeed cubelike. Moreover, the nanocubes obtained from this approach are very uniform in size. This will be further evidenced with our quantitative image statistics (next subsection). It is also interesting to note that during the tilting experiments, some equispaced fringes can be seen in the areas where two nanocubes overlap (e.g., Figure 3d). Because their spacing is much larger than any expected inter-planar distances of Co_3O_4, they are assigned to intersected fringes of the two sets of crystallographic planes (each belongs to a nanocube), as commonly observed in highly crystalline materials with TEM technique.

Size-Controlled Growths. Use of an excessive amount of salt (sodium nitrate in this case) is essential to obtain the nanocubic Co_3O_4.[32] Without sodium nitrate, it was found that the intermediate product cobalt hydroxide nitrate, $Co^{II}(OH)_{2-x}(NO_3)_x \cdot nH_2O$, was missing from the reaction mixture. In that case, only β-$Co(OH)_2$ and hydrotalcite-like cobalt double hydroxide, $Co^{II}_{1-x}Co^{III}_x(OH)_2(NO_3)_x \cdot nH_2O$, are converted to spinel oxides after prolonged reactions.[32] It is thus postulated that the competitive presence of the nitrate salt is responsible for modifying the chemical route; that is, a large amount of nitrate anion competes with OH^- to form a new precursor phase, $Co^{II}(OH)_{2-x}(NO_3)_x \cdot nH_2O$.[32] Owing to the "salting-out" effect,[36-38] solubility of oxygen in synthetic solution is reduced, which delays the above hydroxide and hydrotalcite-like compounds to Co_3O_4 conversion. Furthermore, formation of salt−$(solvent)_n$ clusters,[39] which act as an additional diffusion boundary on the resulting Co_3O_4 nanoparticles, is believed to regulate the faceting of spinel oxides nanoparticles.[32]

With the increase in reaction temperature in this work, formation of Co_3O_4 nanocubes has been significantly accelerated. For example, Co_3O_4 nanocubes in the size around 43−45 nm can be attained with only 12 h reaction at 105 °C [instead of 48 h at 95 °C in our previous work (ca. 47 nm)[32]]. Furthermore, owing to the faster reaction rate, the size of these nanocubes can be controlled more easily with a simple variation of reaction time (or aging time). In fact, we have obtained nanocubes as small as 10.6 nm (average edge length) with a standard deviation of 1.4 nm when the aging time was 3 h, as reported in Figures 4a and 5a (also Table 1), noting that some of these nanocubes can self-align into 1D arrays (framed parts) owing to presence of their intrinsic magnetic diploes. On the basis of the TEM image statistics it is found that the amount of nitrate salt used (either 90 or 150 g) does not cause a substantial influence on the sizes of the nanoparticles. However, it does cause some subtle variations in growth habits (which will be addressed soon). With only 3 h reaction, these Co_3O_4 nanoparticles have started to show cubic type morphology, although they are not as well-faceted as samples obtained with longer aging times. It is also worthwhile to note that the acidic washing treatment was essential to harvest these small particles because the yield of cobalt spinel was very low at this stage. In principle, it is possible to capture even smaller particles by drawing samples at even shorter aging times. However, the extremely low yield makes it impractical to do so. Nonetheless, the possibility of synthesizing even smaller (a few nanometers) and yet uniform nanocubic cobalt spinel oxide is positively indicated. With the aging times of 6 and 12 h (Figures 4b and c and 5b and c), the particles are gradually grown in size and are better faceted. As evidenced in Figure 6, the size kinetics appears to be linear with respect to time and independent of the amount of salt added under the synthetic conditions investigated (i.e., 90 g of $NaNO_3$ has been sufficient to generate the cubelike morphology). Although our primary focus in this work is on the Co_3O_4 cubes in the range of 10−50 nm, this linear relationship is likely to be extended to 100 nm (e.g., Figure 3a, ca. 100-nm cube-edge with 24 h reaction time). To understand the evolution of the particle size with time, the statistical analysis of particle size is further reported in Table 1. Although the size of the nanocubes increases with time, the percentage deviation does not, which indicates an improvement in size uniformity for the long-aged samples. In this agreement, 2D assemblies of Co_3O_4 nanocubes can be commonly observed even without assistance of surfactants (e.g., Figure 4b and c).

Table 1. Statistical Analysis of the Co_3O_4 Nanocube Size (Edge Length)

aging (h)	mean size (nm)	standard dev. (nm)	percent dev. (%)
90 g of sodium nitrate used			
3	11.2	1.6	14.3
6	24.3	2.1	8.7
12	44.7	2.8	6.3
150 g of sodium nitrate used			
3	10.6	1.4	13.2
6	25.3	1.7	6.7
12	43.1	3.7	8.6

Growth Mechanism. Chemically, we have understood in our previous work the phase-evolution process of Co_3O_4 nanocubes.[32] On the basis of our present new findings, the growth mechanism of the nanocubic spinel will be addressed further, though it is yet difficult to establish a quantitative kinetic model at this stage.

In Figures 4 and 5, a considerable amount of Co_3O_4 nanoparticles (marked with an arrow) show peculiar

(36) Elliot, A. J.; Chenier, M. P.; Ouellette, D. C. *Fusion Eng. Des.* **1990**, *13*, 29.
(37) Schumpe, A. *Chem. Eng. Sci.* **1993**, *48*, 153.
(38) Tan, Z. Q.; Gao, G. H.; Yu, Y. X.; Gu, C. *Fluid Phase Equilibr.* **2001**, *180*, 375.
(39) Dedonder-Lardeux, C.; Gregoire, G.; Jouvet, C.; Martrenchard, S.; Solgadi, D. *Chem. Rev.* **2000**, *100*, 4023.

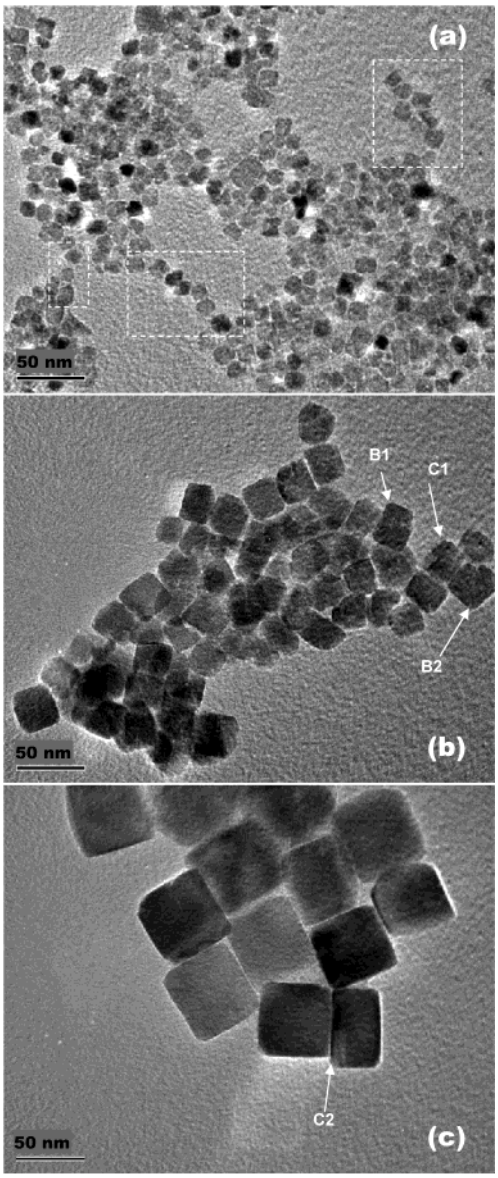

Figure 4. TEM images of Co_3O_4 nanocrystallites prepared with addition of 90 g of $NaNO_3$: (a) aging time 3 h; (b) aging time 6 h; and (c) aging time 12 h. Some marked crystallites will be addressed in Figure 7.

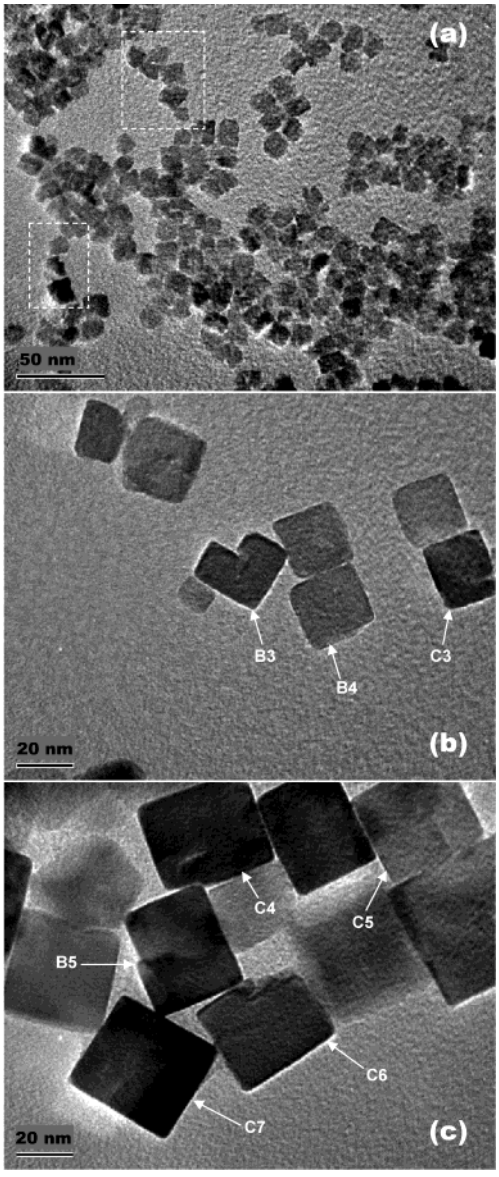

Figure 5. TEM images of Co_3O_4 nanocrystallites prepared with addition of 150 g of $NaNO_3$: (a) aging time 3 h; (b) aging time 6 h; and (c) aging time 12 h. Some marked crystallites will be addressed in Figure 7.

morphologies, although the majority of the Co_3O_4 crystallites are highly symmetrical nanocubes with equal edges. Owing to the significant increase in growth rate at 105 °C, the growth fronts of these intermediate nanoparticles have been amplified (i.e., a better faceting is attained) and hence become more observable, especially in the growths in which $NaNO_3$ was heavily loaded (150 g, Figure 5). Apart from the normal "perfect" nanocubes (A type), basically, there are two types of "abnormal" growing cubes. As illustrated further in Figure 7, the first one — B type (e.g., B1−B5, Figures 4 and 5) — indicates some sidewall propagation, whereas the second one — C type (e.g., C1−C7, Figures 4 and 5) — belongs largely to an in-plane completing growth.

As all crystallites observed can be broadly classified into one of the types A, B, or C, a correct sequential arrangement of these crystallite types would naturally disclose the nano-cubic Co_3O_4 growth mechanism. Regarding this arrangement, surprisingly, we do not have much choice, but to come up with a "surface wrapping" growth mechanism as depicted in Figure 7. This model

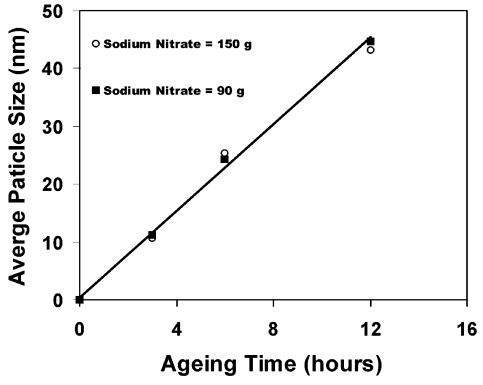

Figure 6. Average size of Co_3O_4 cube edges as a function of aging time and nitrate salt added. The line is linearly fitted with $R^2 = 0.997$.

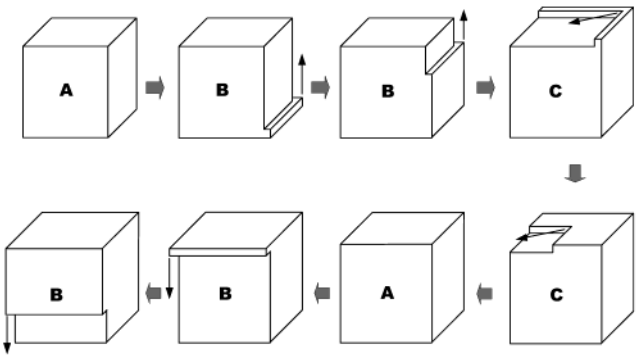

Figure 7. Schematic illustration of "surface wrapping" growth mechanism based on the morphologies of intermediate crystallites (B and C) observed. Arrows indicate the advancing directions of small crystal planes (growing surface "shells", see text). The crystallite types of B and C can be referred to the marked crystallites in Figures 4, 5, and 9.

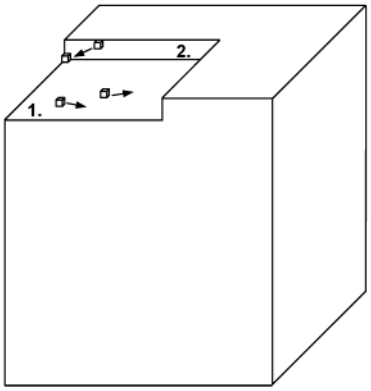

Figure 8. Small and large crystal planes in type C crystallite (marked areas "2" and "1", respectively). Growth entities are indicated with little cubes moving on the crystal planes; arrows indicate their moving directions.

gives a logical repetition of the three types of nanocrystallites, i.e., ··· → A $_{\text{smaller}}$ → B → C → A $_{\text{larger}}$ → ···, while the overall structural isotropy is strictly maintained during the cube growth. The interchange between B and C is also equally plausible. But prior to a next greater crystal, a smaller A-type crystal has to go through both B and C stages in order to sustain the isotropic growth. In this sense, an original crystallite A seems to be wrapped with new Co_3O_4 surface "shells" when it goes through B and C.

It is important to note that the height of these "shells" is in the range of a few nanometers, which is apparently much higher than any atomic steps on the {100}, {010}, and {001} surfaces of Co_3O_4. Unambiguously, the present growth does not proceed in a (atomically) layer-by-layer manner but with a multiple-layer growth, i.e., nucleation and growth are taking place simultaneously in different atomic layers. In this regard, one should view these growing "shells" as small advancing crystal planes (or growth fronts). Illustrated in Figure 8, one could realize that the formation of small crystal planes (area 2) within a cube surface actually increases the total surface area. Furthermore, more ledges and kinks can be generated on the small crystal planes (area 2) than on the large planes (area 1). By creating these small crystal planes, the growth entities could be better accommodated, as their diffusion distance to a nucleation site is greatly shortened.

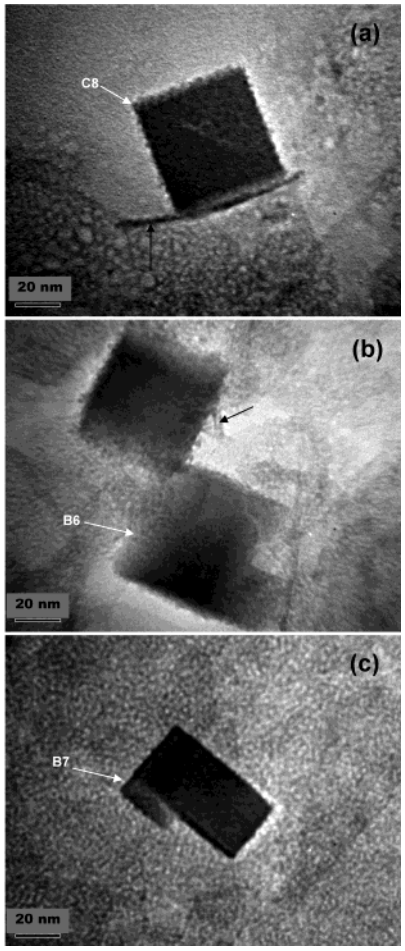

Figure 9. TEM images of Co_3O_4 nanocrystallites together with the layered compounds $Co^{II}(OH)_{2-x}(NO_3)_x \cdot nH_2O$ and $Co^{II}_{1-x}Co^{III}_x(OH)_2(NO_3)_x \cdot nH_2O$ (as backgrounds; black arrows in (a) and (b) indicate the layer-attachment to the growing cubes). The sample was prepared with addition of 150 g of $NaNO_3$ and an aging of 12 h. Note that the sample was washed thoroughly with deionized water (but without using acid HCl). Marked crystallites in (a) to (c) can also be referred to Figure 7.

Finally, we must ensure that the above observed growth fronts were not created by the acid washing. Figure 9 shows three TEM images for Co_3O_4 nanocubes together with the sheetlike precursor compounds without the acid washing. It is interesting to note that the surfaces of growing nanocubes are not so smooth. Presumably, they are covered with fragments of the decomposing basic compounds[32] that can be dissolved in the HCl solution during the acid washing. In many cases (Figure 9a and b), larger sheets of the solid compounds are attached on the surfaces, which may indicate some electrostatic interactions between the cube surfaces and the layered compounds when they undergo the nitrate anion deintercalation, although actual processes are still not clear at this time. Nonetheless, the intermediate cubes and their growing fronts illustrated in Figure 7 are indeed present during the growths (marked crystallites C8, B6 (viewed along [110]), and B7, Figure 9). Understanding the above growth mechanism would allow us to control the nucleation and/or to grow the Co_3O_4 nanocubes with atomic flatness. In principle, the multiple-layer growth can be suppressed by controlling the degree of supersaturation

of solution and lowering the reaction temperature. We are currently working along this direction.

Conclusions

In summary, by controlling reaction temperature and time, the size of our previously prepared Co_3O_4 nanocubes can be further reduced down to the range of 10−50 nm with high crystallite-monodispersivity. Using the present approach, the relationship between the cube-size and reaction time is linear. Furthermore, it has been proven in this work that the separation of the growing Co_3O_4 nanocubes from the remaining solid products can be easily achieved with acid washing (2.0 M HCl solution in the current case). Under the assistance of nitrate salt to the growth, irregularly faceted crystallite intermediates can be preserved, which leads us to elucidate a "surface wrapping" growth mechanism for the formation of Co_3O_4 nanocubes. The growth synthesis of Co_3O_4 nanocubes is a multiple-layer type. Apparently, under the present higher supersaturation condition, growth entities can be better accommodated on the smaller growth fronts perpendicular to the cube surfaces.

Acknowledgment. We gratefully acknowledge the research funding (R-279-000-064-112 and A/C50384) co-supported by the Ministry of Education and the National Science and Technology Board of Singapore.

CM020940D